SOME STUDIES ON REGENERATIVE BEAM EXTRACTION IN SYNCHROCYCLOTRONS

S. Kullander*), S. Lindbäck, Å. Svanheden
The Gustaf Werner Institute,
University of Uppsala, Sweden

Abstract

In this paper it is shown that the extraction efficiency in a synchrocyklotron can be increased considerably by selecting proper values for the internal circulating beam parameters. A good energy homogeneity and a high microscopic duty cycle can be achieved simultaneously. A calculation for some relevant radial amplitudes and energy gains/turn gives the energy diagram in fig. 11. From this it can be found that, if the internal beam is composed of 0.4 - 0.6 cm incoherent radial amplitudes and if the useful acceleration voltages are 7.2 - 10.6 kV, the gross extraction efficiency is 40 % for an energy spread of 300 keV. The duty cycle will be about 20 %. These results are valid if the vertical amplitudes are small so that the median plane motion program is correct.

- - - - - - - - - - - - - - - - - - -

Introduction

In a regenerative extraction system[1-5] the extraction efficiency, η, depends critically on the quality of the internal circulating beam. In a synchrocyclotron η is usually very low. It has been found, however, that this extraction method can give a duty cycle of 25 %[6] and an energy spread of 0.2 MeV (FWHM) at 185 MeV[7] protons.

In order to study the influence of radial and phase oscillation amplitudes on the regenerative process and to find suitable dee-voltages, computer calculations have been performed in which the particles were followed during the whole extraction process. Below will be given explanations for the behaviour of the particles during the extraction process and for the compression of the energy spread that takes place[8]. Finally it will be shown how a large gain in extraction efficiency, keeping the small energy spread, can be accomplished by an adequate choice of the internal circulating beam parameters.

The beam extraction of the Uppsala synchrocyclotron

In 1955 the beam was successfully extracted from the cyclotron by adopting a non-linear regenerative system. The extraction was considered to start at a radius r_g = 100 cm, and the beam had to pass a magnetic ridge of about 12 cm radial width before it could spiral out. The maximum useful radius was 102 cm where the field index n = 0.2. After passing a magnetic channel at r = 108 cm the phase-space distribution of the beam was changed by two "focusing channels" in the fringing field, as is shown in fig. 1. The extraction system is found to be very energy selective and only a small fraction of the internal circulating beam passes. Typically, the energy spread is 13 MeV FWHM at 180 MeV, as was measured by using the cyclotron magnet as a 180° analyzer. The energy spread in the external beam has been measured to be not more than 0.2 MeV FWHM, and the extraction efficiency is normally 1 %. However, by changing the ion source conditions yielding a reduced intensity of the internal circulating beam, the extraction efficiency can be increased to a few percent. Separate measurements have shown that the energy spread in the internal circulating beam is decreased under these conditions. These measurements indicate that the extraction system accepts only relatively small amplitudes of the radial oscillation, as will be shown to some extent below. The external cyclotron beam is brought through an evacuated tube of about 20 meters length to the experimental area, where the beam can be focused by a quadrupole pair to a cross section of about 10 mm^2. The emittance is about 230 mm.mrad in both planes, and the intensity is normally $5 \cdot 10^{10}$ protons/sec.

Median plane motion

Assume that the regenerator field and the fringing field start at the same radius r_g. The radius of the equilibrium orbit for a particle moving in the field, and the amplitude and angular frequency of the betatron oscillation are denoted by r_o, ρ_m and ω_r, respectively, where ω_r is given by

$$\omega_r = \omega(1-n)^{1/2} \qquad (1)$$

The maximum radial outswing ($r_o + \rho_m$) at azimuth θ_m will precess around the magnetic centre of the cyclotron and the same holds for the orbit centre P. The locus of the precession of P is essentially a circle with radius ρ_m (1-n). As soon as the regenerator field starts to influence the particle motion for some value $\theta_m < \theta_r$, θ_r being the regenerator azimuth, there is a certain increase in ρ_m per turn, as is shown in fig. 2. If the particle has not penetrated enough, P will "slip" past the regenerator azimuth and ρ_m starts to decrease. Due to the successive increase in r_o caused by the acceleration, the regenerator action is on the average stronger for $\theta_m > \theta_r$ than for $\theta_m < \theta_r$, and this implies that a slip through the regenerator always causes a net decrease in ρ_m, which will somewhat affect

*) At present at the European Organization for Nuclear Research (CERN)

the energy compression, as will be discussed later. The most critical passage at the regenerator is when $\delta\theta_m$, the total slip in θ_m per turn, is almost zero. This gives a slow precession during which much energy is gained, i.e., r_o increases thus giving a strong regenerator action for $\theta_m > \theta_r$ and a considerable decrease in ρ_m. During the last stage of the extraction the motion of the particles is strongly locked in phase by the extraction system, i.e., θ_m is fixed at some value θ_f ($\theta_f < \theta_r$). The motion of θ_m (or P) towards θ_f can proceed in mainly two different ways. For particles experiencing a relatively weak regenerator action $\delta\theta_m \to 0$ for $\theta_f < \theta_m < \theta_r$, which means that θ_m will decrease and return to θ_f, giving the motion of P in the $\rho_m\theta$-plane the characteristic form of a "knee". For particles experiencing a relatively strong regenerator action, $\delta\theta_m$ is always positive and θ_m approaches θ_f from smaller values, which gives a more "straight" extraction. This can be seen in fig. 3, which is a result of a computer run. Particles A and B belong to the latter category and D and E to the former.

In the following is developed a theory for the motion of the orbit centre P. We start at the moment the particle crosses r_g on the entrance to the linear field region and assume that this happens at $\theta = \theta_r$. One revolution later the particle will experience regenerator action and ρ_m will increase by an amount of $\delta\rho_m$. The quantity $\delta\rho_m/\delta_m$, expressed as a function of the parameters $b = r_o - r_g$, θ_m and ρ_m, determines how strongly the extraction sets in, and, as the regeneration process is cumulative, the value of $\delta\rho_m/\rho_m$ should give a good idea of the subsequent motion of P. For particles with the same $\delta\rho_m/\rho_m$ the trajectories described by P will be approximately uniform, if an essentially constant accelerating voltage (small phase oscillations) is assumed. In order to get an expression for $\delta\rho_m/\rho_m$ we define $x = r - r_g$ and $\theta_d = \theta_r - \theta_m$. If ν_o is the betatron frequency corresponding to the equilibrium orbit r_o, the increase in θ_m due to the precession is

$$\delta\theta_{mp} = \frac{2\pi\ (1-\nu_o)}{\nu_o}$$

The radius of the precession circle is $\rho_m(1-n) = \rho_m\nu_o^2$ and consequently the vector $\underline{F}_1$ in fig. 2 is

$$F_1 = \delta\theta_{mp} \cdot \rho_m\nu_o^2 = 2\pi\ \nu_o(1-\nu_o)\rho_m$$

After one revolution the outswing x_r in the regenerator becomes

$$x_r = 2\pi\ \nu_o\ (1-\nu_o)\rho_m \sin\theta_d + \delta r_o \qquad (2)$$

as can be found from fig. 2. The first term is thus caused by the precession and the second term is the increase in r_o due to acceleration. The increment $\delta\rho_m$, caused by a regenerator of strength $Tx_r + Wx_r^2$ ($\underline{F}_2$ in fig. 2) is roughly

$$\delta\rho_m = (Tx_r + Wx_r^2) \cdot \sin\theta_d \qquad (3)$$

Inserting eq. (2) in eq. (3) gives (neglecting the second order term in δr_o)

$$\delta\rho_m/\rho_m = Tc_1 \sin^2\theta_d + Wc_1^2\rho_m \sin^3\theta_d +$$

$$+ \delta r_o\left(\frac{T}{\rho_m} \cdot \sin\theta_d + 2c_1W \sin^2\theta_d\right) \qquad (4)$$

where

$$c_1 = 2\pi\nu_o(1-\nu_o)$$

The first and second terms in (4) arise from the linear and quadratic terms, respectively, of the regenerator strength. The third term represents the contribution due to the acceleration. Since δr_o is small compared to T, W and c_1 it is seen that the third term is important only for small ρ_m. Graphs of $\delta\rho_m/\rho_m$ for $\rho_m = 0.2$ cm and 1.0 cm are shown in fig. 4. The relation at the starting moment between b, ρ_m and θ_d can be found from geometric considerations which yield

$$\cos\theta_d = \frac{-b}{\rho_m \cdot \nu_o^2} \qquad (5)$$

and this relation is shown in fig. 5 with b as parameter. Lines of constant value of $\delta\rho_m/\rho_m$ in fig. 4 give a relation between ρ_m and θ_d at the points of intersection with the curves. Plotting these points in fig. 5 and joining points of constant $\delta\rho_m/\rho_m$ one gets what may be regarded as equipotential levels for the relative strength of the regeneration. One of these levels forms the threshold between slip and knee motion. In fig. 5 the position of the orbit centre for a sample of numerically traced particles is marked when $x_r = 0$, i.e., when the particles reenter the linear field at the regenerator. Dots indicate that slip motion will follow and circles and triangles indicate knee and straight extraction, respectively. In order to trace some interesting particles from the slip position to the final regeneration state in the diagram, connecting lines have been drawn. Those lines "cover" the 30 - 40 turns needed for the last betatron cycle and they show the decrease in ρ_m associated with a slip motion. The threshold level in this analysis is calculated by the computer and is shown in the diagram (upper "computed" curve). As a comparison the analytically calculated curve is also given, the position of which is chosen to be common with the computed curve for $\rho_m = 0.6$. Just below the threshold level there is a critical interval where the particles get a slow, attenuated precession. Particles occuring in this interval suffer a considerable decrease in amplitude and an excessive energy gain when slipping and even if all the

incoherent particles in the internal circulating beam initially have the same radial amplitude, it is impossible to avoid a range of amplitudes (almost down to zero), when the particles finally regenerate. This gives rise to an increased energy spread in the beam. The motion of P, for some representative particles A, B, D and E has already been shown in fig. 3 and the same particles are marked in fig. 5. Note the strongly pronounced knee motion for particle E, which starts just above the slip threshold, and turns at $\theta_m = \theta_r$. Consequently for small amplitudes particles closer to the threshold can be captured although θ_m has passed θ_r. Particle A, first appearing in the critical interval, slips and is later on extracted straightly.The curve defining the lower limit of this interval is computed for particles having a slip of 2.8°/turn when P passes θ_r.

An accelerating voltage of 20 kV gives an average increase in b of about 0.35 cm per betatron cycle. A particle accelerated with a lower voltage has a slower "motion" through the slip region towards the extraction region (above the threshold) which can be found from fig. 5. This effect increases the probability of getting the particle into the critical interval, which gives rise to an uncontrolled energy spread during the extraction process. Hence, large phase oscillations are disadvantageous.

Energy compression

In order to understand the factors causing the energy compression during the extraction we divide the whole regeneration process in two parts. The first includes the particle motion to the final regeneration state, and the second the final regeneration (knee or straight). During the first part the energy is compressed due to the fact that particles with larger amplitudes make more precession cycles, which can be found from the position of the threshold level in fig. 5. For example two amplitudes 0.2 and 1.0 cm, initially differing 0.8 cm in r_o, can differ from 0.35 to 0.65 in r_o when the knee region is reached. During the second part of the regeneration state energy compression occurs for particles having the same amplitude (or lying within a narrow band of ρ_m) while a certain decompression takes place if a large range of amplitudes are present. This can be found from eq. (4). If $\rho_m \simeq$ const., $\delta\rho_m$ increases with θ_d, i.e., with r_o and thus particles with large energy escape after fewer turns. If $\theta_d \simeq$ const., $\delta\rho_m \sim \rho_m$ (approximately) and thus particles with larger ρ_m escape faster. But since $\theta_d \simeq$const. means a smaller r_o for increasing ρ_m (fig. 5) we conclude that the energy difference between particles with small and large ρ_m has increased when escape occurs. This decompression, however, is smaller than the compression during the first part of the regeneration and hence there is in general a net energy compression which is larger the samller is the range in ρ_m when the final regeneration starts.

Numerical results

In the program set up in order to study the particle motion, accelerated particles are followed from the instant the maximum radial outswing reaches $r = r_e$. Due to the incoherent radial amplitudes, this can occur at any azimuth θ_{mi}. The acceleration and the motion in electric phase space are included. The electric phase at start, the synchronous phase and the phase oscillation amplitude, as well as the dee voltage, are parameters of the program. Thus one has complete freedom in choosing the initial conditions. The magnetic fields are approximated by analytical functions. The fringing field in the median plane is described by a hyperbola and the regenerator field by a parabola given by LeCouteur's parameters T = 0.2 and V = 0.08. The azimuthal distribution of the regenerator field is rectangular ("hard edge") and has a length of 12° (21 cm). In fig. 6 ρ_m as a function of the number of turns, N, is shown for 6 particles with representative initial amplitudes, all particles starting with P at the same azimuth. A maximum energy gain per turn of 40 keV and an electric phase at start of 50° yield the equilibrium orbit expansion $\Delta r_o(N)$, which is slightly curved due to the phase oscillation. Particle A starts the final regeneration when N = 10. Because B - F start at the same azimuth as A, they are all influenced by the regenerator when N = 10, at which time B- F are well below the threshold. Therefore they make another precession cycle, after which they reenter at N = 40 and experience a stronger regenerator action than previously because of the increase in r_o due to the acceleration. Now B - E regenerate while F, just below the threshold, slips over the regenerator for a new betatron cycle. Therefore the precession is slow at the passage, and due to this, particle F finally regenerates with a comparatively greater energy increase than the other particles. It can be seen from the table in fig. 6 that an initial energy difference of 2.83 MeV is reduced to 1.60 MeV for the particles A - F. In fig. 7 the corresponding $\rho_m(\theta_m)$ plots are shown. Particle A, having an extraordinary knee motion, spends about 40 turns in the final regeneration state. Particle B regenerates straight in around 15 turns. The other particles exhibit knees of different magnitudes. For all of them θ_m approaches θ_f asymptotically.

Due to the incoherent radial oscillations and due to different acceleration histories, particles which initially had the same amplitude can start the final regeneration with a range of r_o-values. If r_{o1} is the value of r_o at this moment, the number of turns N_1 needed for a particle to escape depends on r_{o1} as explained earlier. A small r_{o1} was found to correspond to a large N_1 depending on the knee motion. Hence it is expected that the energy spread due to different entry values of r_{o1} could be made small by a proper choice of the accelerating voltage. Large phase oscillations, yielding a large range of

r_o, are certainly harmful in this respect. The quantitative behaviour in the final regeneration state is best seen from the $N_1(r_{o1})$ diagram in fig. 8. The diagram has been constructed using the data collected for a number of incoherent particles traced through the extraction system; δr_o has been chosen to 0.01 cm. The parameter ρ_{m1} is the value of ρ_m at $r_o = r_{o1}$. A particle with r_{o1} corresponding to the portion of the curve where dr_o/dN is small regenerates with the centre of curvature making a knee motion in the $\rho_m\theta_m$-plane. Particles starting the regeneration in this region need a relatively small δr_o to homogenize the final energies. The arbitrary choice of δr_o does not appreciably change the $N_1(r_{o1})$ plots, because the particle trajectories are not very sensitive to the acceleration voltage, when the regeneration is once initiated. On the other hand, the final energies are affected greatly by this choice. Particles occurring on the portion of the curves, where dr_o/dN is large, regenerate straight. Particles entering with these large r_{o1} need between 15-20 turns to regenerate. In order to get a homogenized final energy, 56 kV dee voltage will be needed in this region. This is too high a voltage for a synchrocyclotron. We conclude, therefore, that the useful energy homogenzing occurs mainly because of the knee motion. Particles making knee motions need relatively small voltages to compensate for the energy spread due to the different entry values of r_{o1}. The $N_1(r_{o1})$ plots are not shown above $N_1 = 36$, at which number the r_{o1} values are approximately 0.01 cm larger than those of the asymptotes which are found from the threshold equipotential line in fig. 5.

The median plane motion program does not account for the good energy selection of the extraction system in the Uppsala machine. A channel 1 cm wide will transmit the particles B, C, E, F as is shown in the emittance diagram in fig. 9, and from the table in fig. 6 the total energy spread is found to be 1.4 MeV, which is more than the corresponding value of the measured 0.2 MeV FWHM. In order to explain the good energy selection the vertical motion must certainly be included. Also recalling the fact that the external proton energy is close to the highest possible determined by the B·r product, we conclude that only particles with small radial amplitudes are extracted.

Choice of the internal circulating beam parameters

The choice of the proper ranges of radial amplitudes and dee voltages yielding a large duty cycle and a good energy homogeneity is based on the following considerations. Three radial amplitudes 0.2, 0.4 and 0.6 cm are examined. Smaller amplitudes than 0.2 cm are not likely to occur and a larger range of amplitudes will not be sufficiently compressed. A sample of particles with the chosen amplitudes and with uniformly distributed values of r_o are shown in fig. 10. The r_o values below the r_1 line are initially at $\theta_m = \theta_r$ one betatron cycle prior to final regeneration. Three accelerating voltages are examined and for all possible combinations of amplitude and voltage the critical intervals are marked (dashed regions). Here $r_o = r_2$ denotes the threshold and $r_o = r_1$ the value which gives a slip $\delta\theta_m$ of 2.8^o/turn, when $\theta_m = \theta_r$. This means a damping of the amplitude by roughly 20 %, considered to be a tolerable limit. The particles occurring inside the critical interval regenerate with final energies which are impossible to control. The critical intervals increase for larger radial amplitudes, and smaller voltages. Each particle is represented by a three character index of which the first denotes the initial radial amplitude, the second gives the distribution of equilibrium orbits, and the third index is related to the voltage. After one betatron cycle the particles appear above r_2 with $r_o = r_{o1}$. The r_{o1} values are calculated by adding the equilibrium orbit expansion during the last betatron cycle to the r_o values below the critical interval. The voltage has to be kept sufficiently low in order to avoid a large increase in r_o, i.e. to prevent the particles from reaching regions in the $N_1(r_{o1})$ diagram where dr_o/dN is large (straight extraction). On the other hand, the voltage must be high enough for as many particles as possible to avoid the critical interval. Furthermore, a large range of voltages is required to yield a good duty cycle. This, however, is in contradiction with the need for a constant voltage as δr_o should be equal to dr_o/dN to compensate for the different values of r_{o1}. The dee voltages 14.4, 10.8 and 7.2 kV have been chosen with the mentioned facts in mind. They correspond to δr_o equal to 0.01, 0.0075 and 0.005 cm, respectively. It is now possible to calculate the final energies as the remaining turns N_1 are known from fig. 8. Since the values of ρ_{m1} in the figure are close to the amplitudes beeing investigated, the curves are quite representative. The calculated final energies are shown in fig. 11. As expected there is an energy spread due to the radial amplitudes. The large voltage values appear to be less useful than the small values. For a certain amplitude there is a correlation between final energy and voltage. This can be seen as a duty cycle limitation, which can be partly overcome if, for example, the two amplitudes 0.4 and 0.6 cm are chosen and if the largest voltage value is excluded. This yields a gross extraction efficiency of 40 % for an energy spread of 300 keV. A duty cycle of 21 % is given by the useful voltage range 7.2 - 10.8 kV. In this investigation the loss to the magnetic channel has been neglected. This loss should, however, not be more than 50 %.

Acknowledgements

The authors wish to express their appreciation to Prof. T.Svedberg and Dr. H.Tyrén for continuous encouragement during the course of work. They also want to thank Mrs L.Borgman and Mrs A. Åström for generously given secretarial help. This work has been financially supported by the Swedish Atomic Research Council.

References

1) J.L. Tuck and L.C. Teng, Chicago Synchrocyclotron Progress Report III, 1950.
2) K.J. LeCouteur, The Regnerative Deflector for Synchrocyclotrons, Proc.Phys.Soc. B64, 1073 (1951).
3) K.J. LeCouteur, Perturbations in the Magnetic Deflector for Synchrocyclotrons, Proc.Phys. Soc. B66, 25 (1953).
4) K.J. LeCouteur, A.W. Crewe and J.W.G. Gregory, The extraction of the beam from the Liverpool synchrocyclotron, Proc.Roy.Soc., A232, 236, (1955).
5) K.J. LeCouteur and S. Lipton, Non-linear Regenerative Extraction of Synchrocyclotron Beams, Phil.Mag. 46, 1265 (1955).
6) H. Tyrén, S. Kullander and O. Sundberg, Conference on high energy cyclotron improvement, Williamsburg, 1964.
7) Å. Svanheden and H. Tyrén, Conference on high energy cyclotron improvement, Williamsburg, 1964.
8) N.F. Werster, The influence of Regenerative Extraction on the energy spread, Sector-focused Cyclotrons, Sea Island Conference, Georgia, 1959.

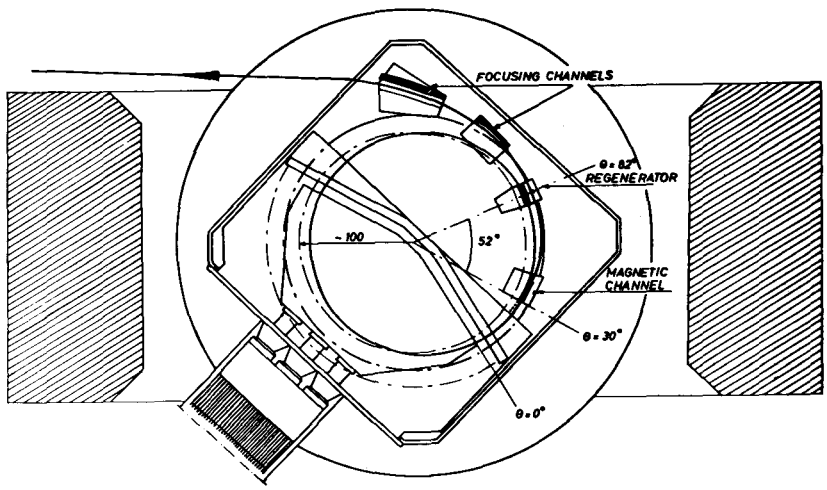

Fig. 1. Lay out of the extraction system for the Uppsala Synchrocyclotron.

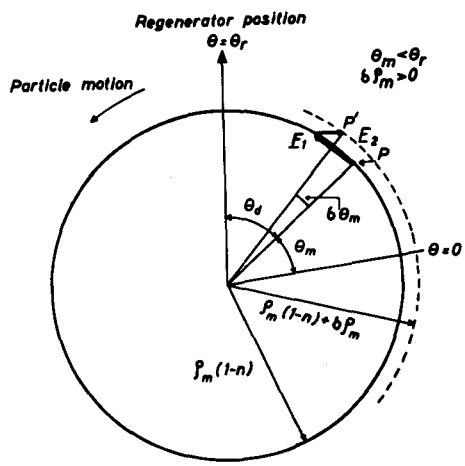

Fig. 2. Motion of centre of curvatures (P) due to precession (F_1) and regenerator action (F_2) during one revolution for the case $\theta_m < \theta_r$. P′ is the new position of the orbit centre.

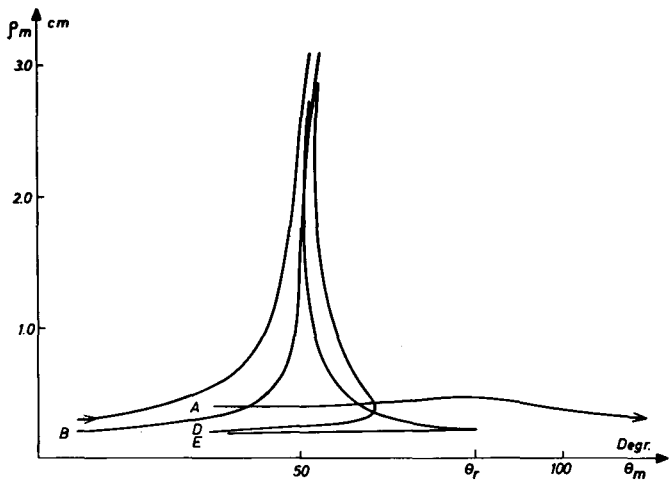

Fig. 3. $\rho_m(\theta_m)$ plots in the final regeneration state.

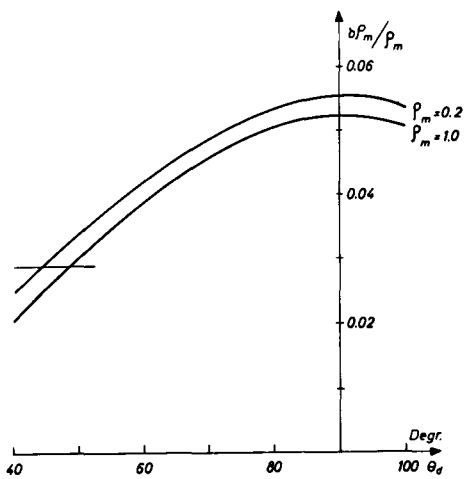

Fig. 4. Curves showing relative increase in amplitude due to regenerator action as a function of θ_d with ρ_m as parameter.

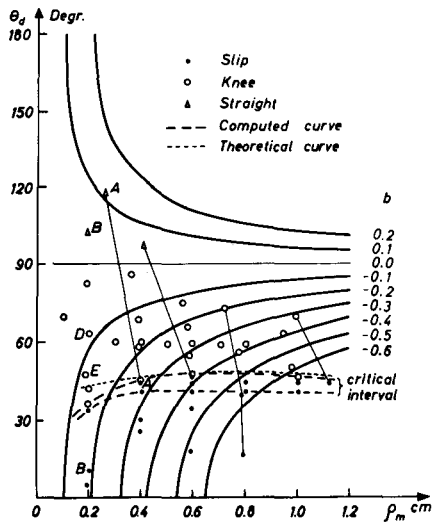

Fig. 5. $\theta_d(\rho_m)$-plots with b as parameter when regenerator action starts (x_r = 0). Solid curves indicate the relations between b, θ_d and ρ_m. Final regeneration occurs above the critical interval.

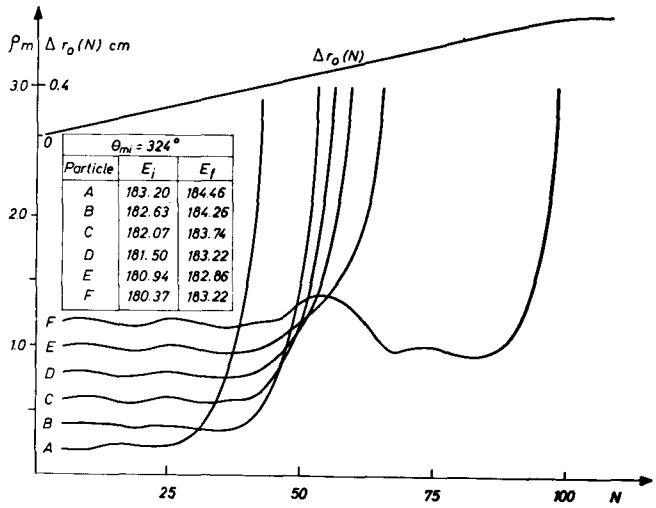

Fig. 6. $\rho_m(N)$ plots. E_i = initial energy. E_f = final energy.

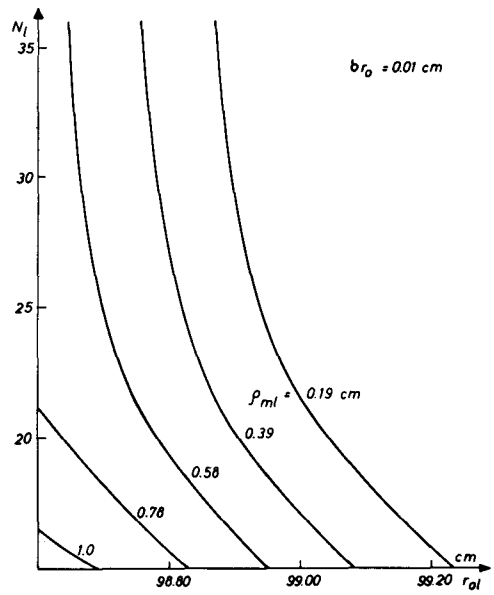

Fig. 8. $N_1(r_{o1})$ with ρml as parameter.

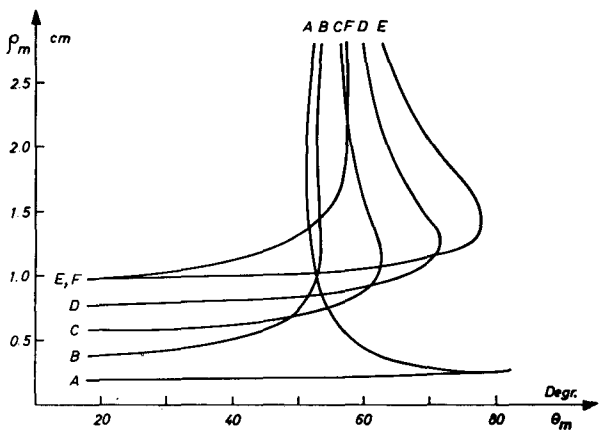

Fig. 7. $\rho_m(O_m)$ plots in the final regeneratoion state for the particles in Fig. 6.

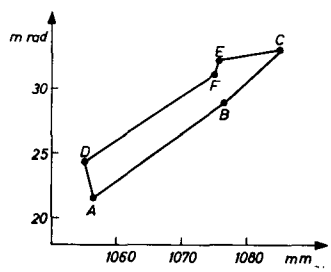

Fig. 9. a) Radial emmitance for particles A - F om Fig. 7.

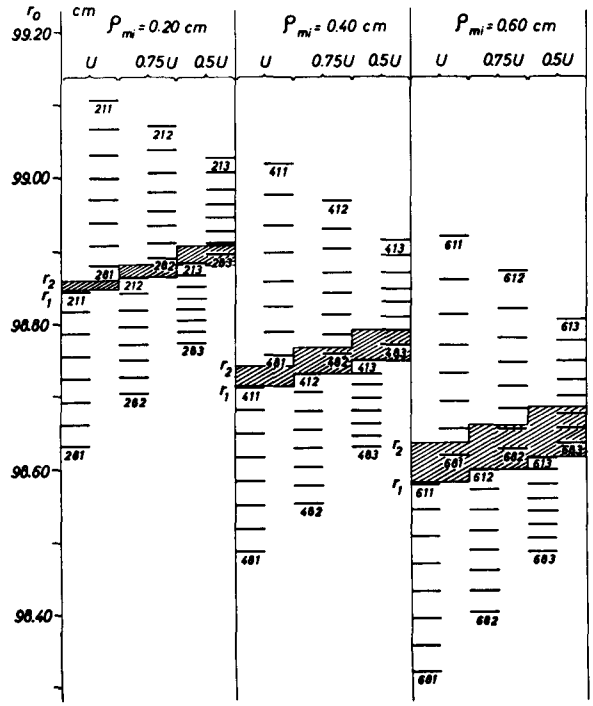

Fig. 10. Level diagram for equilibrium orbits for three different amplitudes and accelerating voltages.

DISCUSSION

HAGEDOORN: Are you concerned about improvements in the central region of the cyclotron to improve the beam quality?

SVANHEDEN: Yes, certainly. Wednesday I will present a paper about our plans for conversion of our cyclotron. We plan to use a calutron ion source, to program all the acceleration process with puller slits, and to combine sector focusing and very small rf band width. If you modulate the rf so as to keep the phase constant during the whole acceleration process, you may end up with small radial as well as small phase oscillations. That should provide for high extraction efficiency from such machines.

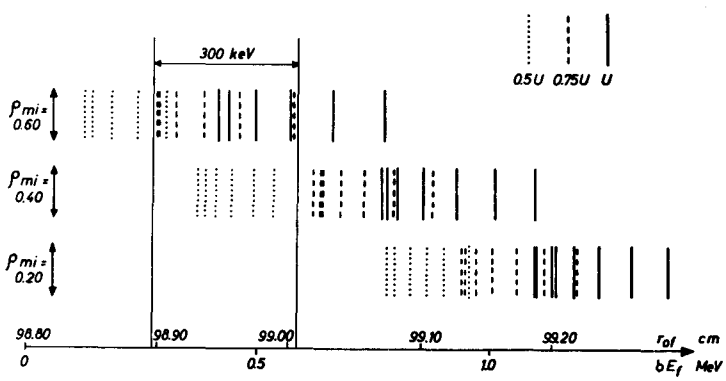

Fig. 11. The final energy distribution for the particles arriving at the magnetic channel.